Available online at **www.joac.info**

ISSN: 2278-1862

Journal of Applicable Chemistry

2019, 8 (4): 1548-1555

(International Peer Reviewed Journal)

Interactions of Green Synthesized Indium Oxide (In_2O_3) Nanofluids with Bovine Serum Albumin Protein

KanchanaLatha Chitturi[1], Aparna Yarrama[1]*, Jinsub Park[2], Dayakar Thatikayala[2], Ramchander Merugu[3] and S. Ramkumar[4]

1. Department of Physics, Nampally, Hyderabad-500001, Telangana, **INDIA**
2. Department of Electronic Engineering, Hanyang University, Seoul 133-791, Republic of **KOREA**
3. Department of Bio Chemistry, Mahatma Gandhi University, Nalgonda-508254, Telangana, **INDIA**
4. Department of Physics, BVRIET, Hyderabad-500001, Telangana, **INDIA**

Email: profyaparna@gmail.com

ABSTRACT

A two-step method which is cost-effective and reliable was used to prepare stable Indium oxide nanofluids by dispersing biosynthesized Indium oxide nanoparticles in ethylene glycol base fluid with a surfactant PVP and Albumin Protein. The precursors Indium (III) Acetylacetonate and Gum Acacia were used for obtaining Indium oxide nanoparticles. The obtained stable nanofluids of Indium Oxide were characterized by Spectroscopy and Microscopy for determining the morphology, size and chemical composition. For different volume concentrations of PVP, the thermophysical properties were studied. It was observed that the effect of PVP and Albumin protein has played a major role on magnitude and behavior of thermal conductivity enhanced about 30% and the decrement in viscosity for 5% volume concentration with that of base fluid at the same temperature.

Graphical Abstract

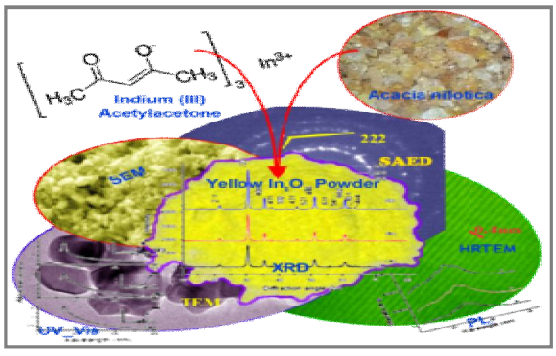

Keywords: Biosynthesis, In_2O_3 nanofluid, PVP, Albumin, Thermophysical properties, TEM, SEM and EDAX.

INTRODUCTION

Nanoparticles dispersion in base fluids like ethylene glycol or water increases the *Thermal conductivity/Viscosity* compared to base fluids. Increase of Thermal conductivity influences the heat engine systems efficiency. Miniaturizations of devices can be applied for industrial cooling [**1-6**].

Inclusion of Polymers and Proteins into the base fluids along with the nanoparticles significantly, is revealing some new properties which are not present in either of the base fluids. In the present work, we used PVP Polymer and the Albumin Protein to study the thermo physical properties, which is the most economic method for the large scale production. The results obtained were correlated and discussed [**7-9**]. Proteins are polypeptides with a defined conformation whose adsorption change to nanoparticle surface changes with changes in pH. PVP and Albumin protein act as efficient agents to improve the stability of suspension [**10**]. Silver nanoparticles in bio-sensing are being investigated due to the optoelectronic properties exhibited by them [**11**]. The adsorption of proteins increase if the surface of the nanoparticles synthesized are curved as they enhance the surface area for binding. Change in the conformation of Bovine serum albumin (BSA) and Cytoskeleton protein tubulin was observed when gold and titanium dioxide nanoparticles were bound to the proteins respectively [**12, 13**]. In contrary, no conformational change was seen when BSA was bound to fullerene nanoparticles [**14**]. Formation of a "hard corona" takes place when proteins bind irreversibly to nanosurface while "soft corona" is seen when binding takes place reversibly [**15-19**]. The above interesting observations made us to investigate the interaction of protein albumin with indium oxide nanoparticles and the results are discussed.

MATERIALS AND METHODS

Fabrication of In_2O_3 nanoparticles and In_2O_3 nanofluid: Eight grams of *Indium (III) acetyl acetonate* purchased from *Sigma-Aldrich* was mixed with 0.8 g of Acacia gum (local Unani Medical Shop at Hyderabad) and were finely powdered using mortar and pestle. The mixture was characterized by TGDTA. The calcination temperature of 400°C was used. After calcining for 2 h yellowish Indium Oxide nanoparticles were obtained. The obtained Indium oxide nanoparticles of 1 % volume were dispersed in Ethylene glycol base fluid. They were sonicated for 30 mins at room temperature. Later surfactant PVP (2 to 5%) was added. The Albumin protein was then sonicated for about 30 min at room temperature after which pH was adjusted (7–8) to obtain Indium oxide nanofluid.

Table 1. Parameters for synthesis of In_2O_3nanofluids

In_2O_3 : PVP : Albumin weight ratio	Description
Sample 1 (1 : 2 : 1)	0.2 g of In_2O_3 with 0.4 g of PVP and 0.2 g of Albumin in 200 mL EG
Sample 2(1 : 5 : 1)	0.2 g of In_2O_3 with 1 g of PVP and 0.2 g of Albumin in 200 mL EG

Characterization of Nanofluids: UV-Vis absorption spectrum (SHIMDAZU), FTIR, RAMAN and PL spectrum, TEM, SEM and EDAX (Hitachi) of Indium Oxide nanofluids were performed to characterize the obtained nanofluids. In the temperature range of 30-60^oC, the density and specific gravity of Nanofluids were measured using ANTON PAAR Density Meter and the viscosity by CANNON-FENSKE Kinematic Viscometer. Electrical conductivity measurements were done with a conductivity meter. Steady state parallel method (Hilton Thermal Conductivity of liquids and gases Unit H471) is used to measure the thermal conductivity of nanofluids. The thermal conductivity can be expressed as shown in Eq.1

$$K = Q_c \Delta r A \Delta t \quad \ldots \text{Eq.1}$$

Where, Q_c–Heat transfers by conduction through the base fluid; $\otimes r$–Radial Clearance, A–Area of conduction path and $\otimes t$ –Temperature difference.

So that the heat transfer co-efficient is in linear behavior with respect to voltage. Nanofluid Interferometer NF-12X is used to measure the ultrasonic velocity, adiabatic compressibility and surface tension.

RESULTS AND DISCUSSION

UV-Vis Analysis: The room temperature UV-Vis absorption spectrum of the In_2O_3 nanofluids is recorded in the wave length range of 200-800 nm. Figure 1 represents the spectrum has a peak at 277 nm (4.4 eV for sample 1 as in table 1) and 287 nm (4.5 eV for sample 2 as in table 2). The absorption peak for 12 nm In_2O_3 nanoparticles has been reported at 270 nm (3.6 eV). The variation in absorption peak is due to the variation of concentration of PVP. Thus at a nanoscale the band gap increases for the In_2O_3nanofluid (sample 2) has excellent stability due to the protection role of PVP and Albumin protein as it prevents the nanoparticles from agglomeration by steric effect [**20**].

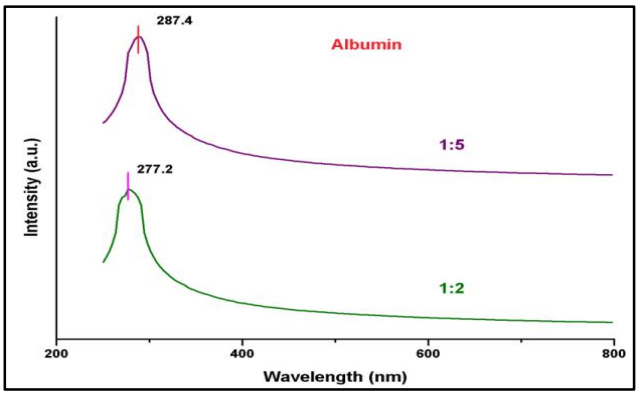

Figure 1.UV-vis absorption spectrum of sample-1and sample-2 of Indium oxide Nanofluids.

EDAX and SEM Analysis: In figure 2, the EDAX spectrum of the In_2O_3nanofluids reveals that the (sample 1 and sample 2) containing '*In*' and '*O*' as main constituent components indicate no contamination is present due to PVP and Albumin proteins and their atomic and weight ratios confirm the literature values. The SEM images of In_2O_3 nanofluids of (sample 1 and sample 2) show the random distribution of nanoparticles having *spherical* shape with porous nature is observed.

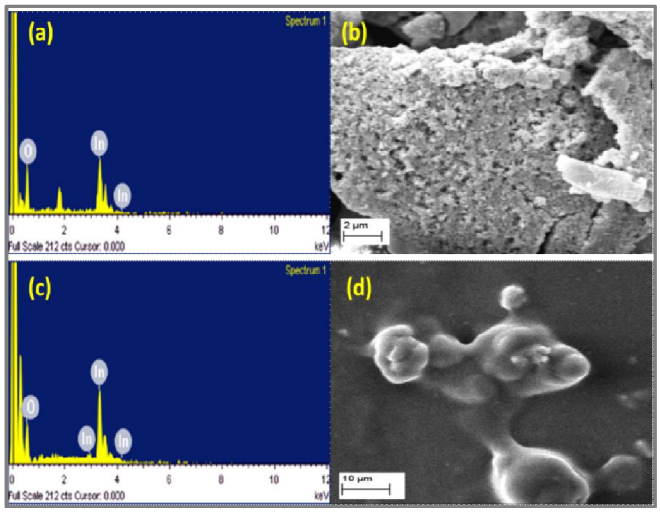

Figure 2. EDAX and SEM of sample-1andsample-2 of Indium oxide Nanofluids.

TEM and SAED Analysis: TEM and SAED images (Figure 3) of sample 1 and sample 2 of In_2O_3nanofluids are depicted which reveal the spherical shape of 10nm size for sample 1 and 20nm for sample 2. The SAED patterns of the two samples reveal polycrystalline structure of In_2O_3

nanoparticles. The interplanar spacing obtained for different *hkl* values are consistent with the *Standard Data* (*JCPDS no.06-0416*) of the two samples as shown in table 2.

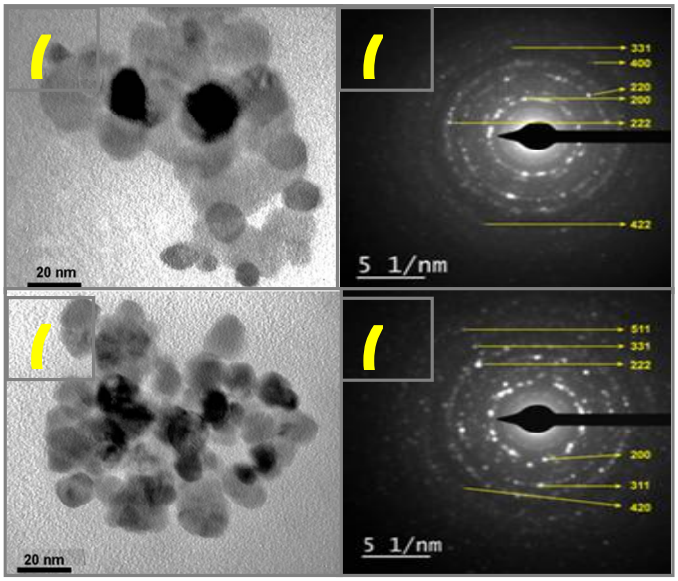

Figure 3. TEM and SAED patterns of sample-1 and sample-2 of Indium oxide Nanofluids.

Table 2. Interplanar spacings of In_2O_3nanofluid (with Albumin protein) from SAED patterns

Ring No.	In_2O_3nanofluid		Standard JCPDS:06-0416	
	Sample 1 d_{hkl}(Å)	Sample 2 d_{hkl}(Å)	d_{hkl}(Å)	*h k l*
R1	1.011	1.035	1.0414	511
R2	1.513	1.5239	1.5622	222
R3	2.888	2.723	2.7056	200
R4	1.887	-	1.9134	220
R5	0.95	-	0.9566	440
R6	1.350	1.395	1.353	400
R7	1.1401	1.124	1.1047	422
R8	-	1.688	1.6318	311

Raman Spectra Analysis: Figure 4 shows the Raman Spectra of sample 1 and sample 2. The expected vibrational modes at 400 cm^{-1}, 861 cm^{-1}, 1100 cm^{-1}. These peaks of samples 1 and 2 confirm the pure In_2O_3 vibrational modes. BSA conformational changes were also seen when they interacted ZnO nanoparticles [21].

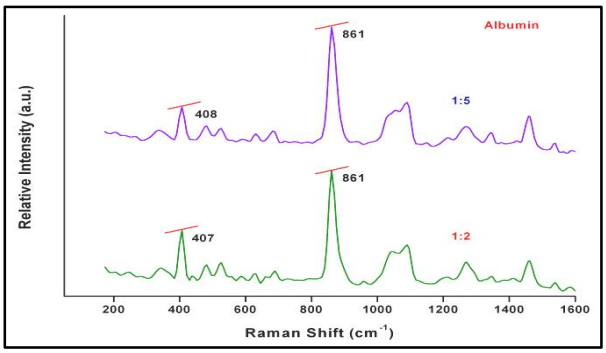

Figure 4. RAMAN spectra of sample-1 and sample-2 of Indium oxide Nanofluids.

FTIR Analysis: IR Spectra of sample 1 and sample 2 (Figure 5) indicates shows the bands around 1650 cm^{-1} (sample 1) and 1652 cm^{-1} (sample 2) which can be ascribed to the C–H vibrations. The absorptions around 1458 cm^{-1} (sample 1) and 1414 cm^{-1} (sample 2) are due to In–O vibrations [22]. Presence of PVP and Albumin on the surface species of the In_2O_3nanoparticles is shown in table 3.

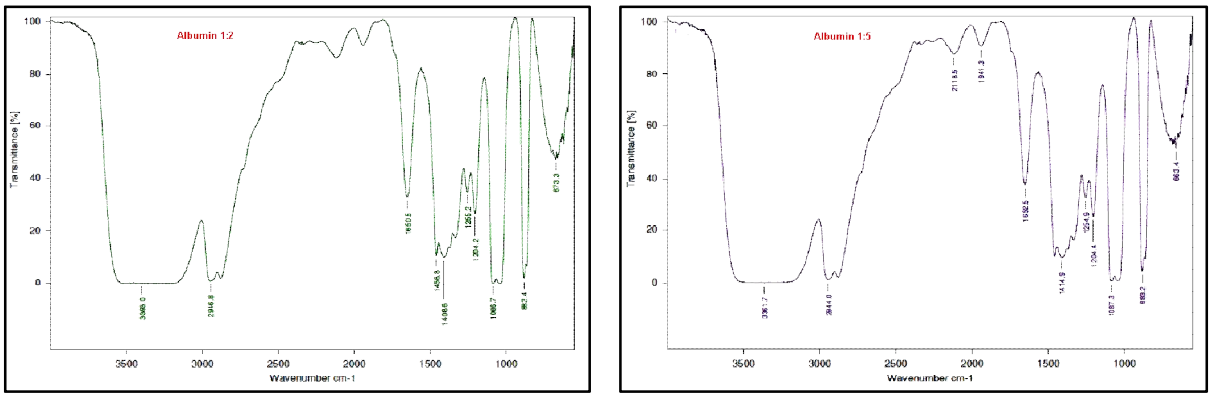

Figure 5. FTIR spectra of sample-1 and sample-2 of Indium oxide Nanofluids.

Table 3. FTIR data of In_2O_3 samples capped with sample1 and sample 2

S.No	C–H Vibration	Adsorption of C=O Vibration	C=O Vibration from Acetyl-acetonate Specia albumin and PVP
Sample 1	2946 cm^{-1}	1650 cm^{-1}	1408 cm^{-1}
Sample 2	2944 cm^{-1}	1652 cm^{-1}	1414 cm^{-1}

PL Analysis: In figure 6, PL Spectra of sample 1 and sample 2 show a weak UV-band at 350 nm and 360 nm respectively. It is well known that a bulk In_2O_3 cannot emit light at room temperature. PL emissions of In_2O_3nanofluid are due to the effect of oxygen vacancies.

Thermo physical properties (TC): Figure 7 represents the voltage versus thermal conductivity. The ratio of K_{eff}/K_b is a non-linear behaviour in sample 1 and a sharp increase with increase of voltage for sample 2 which can be explained by Brownian motion [23]. The enhancement of TC with voltage of sample 2 may be due to polymer and Albumin protein ligand binding, which are considered as important mechanism for enhancing TC of nanofluid [24] and the percentage of enhancement of sample 2 is found to be 30% compared to that of Ethylene Glycol base fluid.

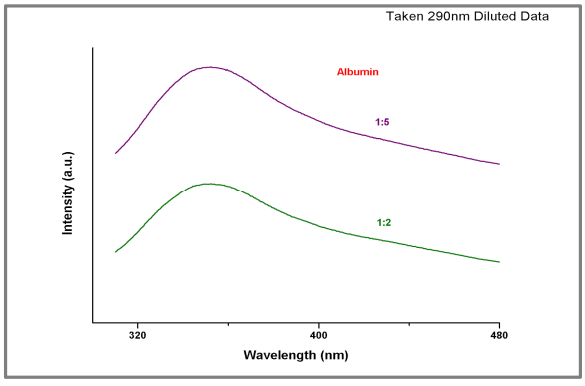

Figure 6. PL Spectra of In_2O_3 samples capped with (a) sample 1 (b) sample 2 at room temperature.

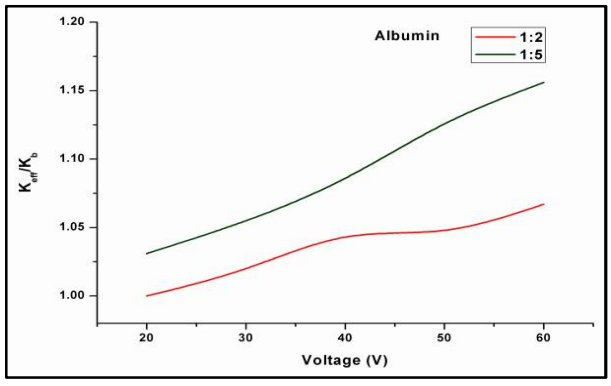

Figure 7. Voltagevs Thermal Conductivity Enhancement Ratio(K_{eff}/K_b) for Indium Oxide nanofluids (sample-1 and sample-2).

Density and specific gravity Analysis: Figure 8 and figure 9 represent the density versus temperature, and specific gravity versus temperature, ranging from 30°C to 60°C increases with increase of concentration of PVP than that of base fluid. Further it is observed that at higher temperature (50-60°C) the sample 2 density and specific gravity decreases.

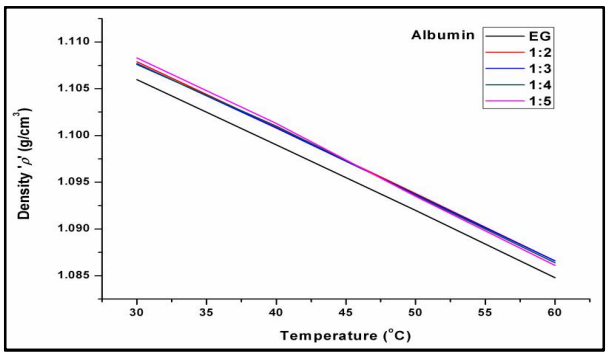

Figure 8. Temperature vs Density of Indium oxide nanofluids (sample-1 and sample-2).

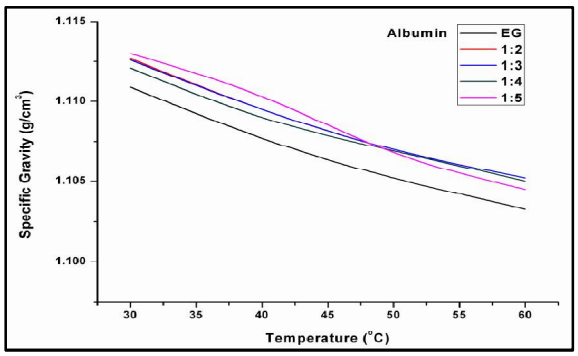

Figure 9. Temperature vs Specific Gravity of Indium oxide nanofluids (sample-1 and sample-2).

Viscosity Analysis: Viscosity vs temperature of different concentrations of PVP Indium oxide nanofluid were analysed and depicted in figure 10. The viscosity of sample 2 decreases with temperature with that of the basefluid ethylene glycol which enhances heat transfer rate.

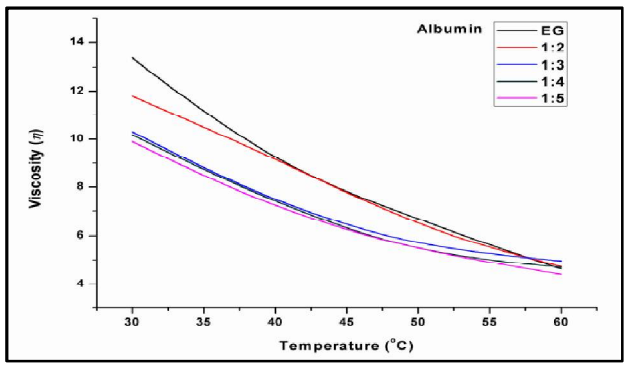

Figure 10. Temperature Viscosity of Indium oxide nanofluids (sample-1 and sample-2).

Ultrasonic Characterization: Ultrasonic velocity of sample 1, sample 2 and basefluid as a function of temperature is shown in figure 11. A non-linear relation between velocity and temperature and is linear at a temperature range of 50°C to 60°C as the concentration of PVP increases the ultrasonic

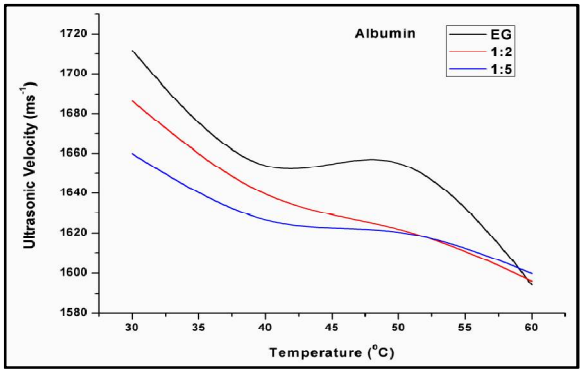

Figure 11. Temperature vs Ultrasonic Velocity of Indium oxide Nanofluids (sample-1 and sample-2).

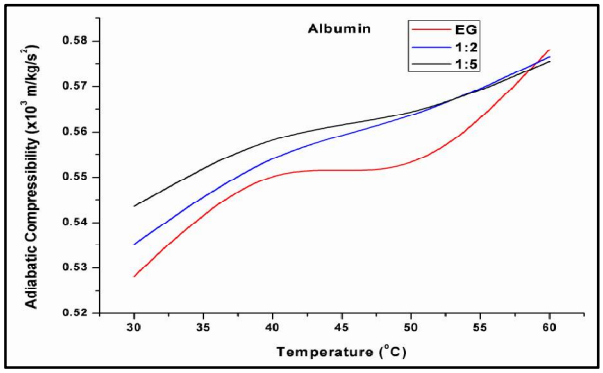

Figure 12. Temperaturevs Adiabatic Compressibility of Indium oxide nanofluids (sample-1 and sample-2).

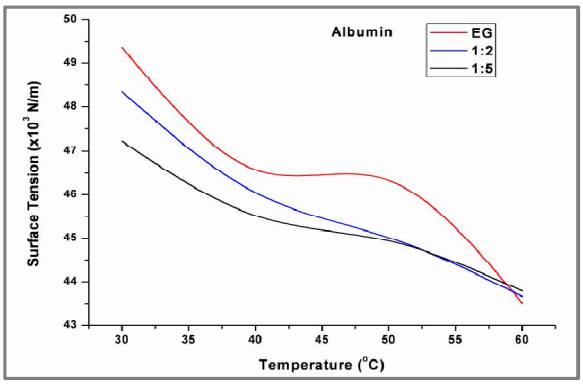

Figure 13. Temperature Surface Tension of Indium oxide nanofluids (sample-1 and sample-2).

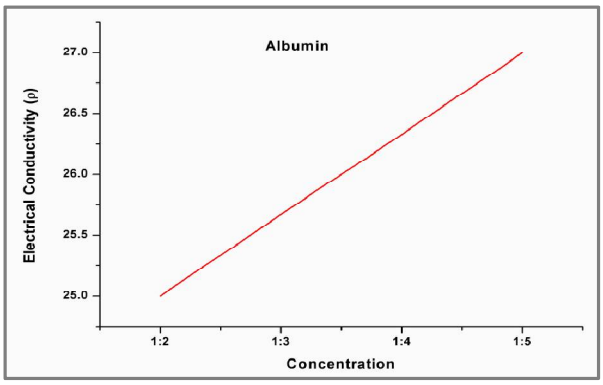

Figure 14. Concentration versus electrical conductivity of Indium oxide nanofluids (sample-1 and sample-2).

velocity increases and adiabatic compressibility (Figure 12) decreases. In figure 13, the surface tension of (sample 2) increases with the increase of temperature than in sample 1 and base fluid confirms that the nanofluids are attributed to surface tension at higher temperatures. In figure 14, the electrical conductivity increases with the increase of concentration of PVP in Indium oxide nanofluid. The order of plasma protein binding to nanoparticles takes place as per Roman theory although for super paramagnetic iron oxide nanoparticle surface this was not obeyed.

APPLICATION

The formation of the nanofluid using Albumen protein can be used as a coolant and reduce harmful emissions from the environment.

CONCLUSION

Successful synthesis of the Indium Oxide nanoparticles and Nanofluids by green and two step method has been presented. Thermal conductivity enhancement and decrement in viscosity with the increase of concentrations of PVP causes heat transfer enhancement which can be applied in industrial cooling.

Conflict of Interest: The author(s) declare(s) that there is no conflict of interest regarding the publication of this paper

Data Availability: All the data which has been obtained through this work has been disclosed in the manuscript.

Funding agency: None but was performed as part of the employment of the authors. The employer is JNTU, Hyderabad, India

REFERENCES

[1]. Trisaksri, Visinee, Wongwises, Somchai. Critical review of heat transfer characteristics of Nanofluids, *Renew SustEnerg Rev*, **2007**, 11, 512-523
[2]. S. Özerinç, S. Kakaç, A. G. Yazıcıoğlu, Enhanced thermal conductivity of nanofluids: a state-of-the-art review. *microfluidics and nanofluidics*, 2010, 8(2), 145-170.
[3]. X. Q. Wang, A. S. Mujumdar, Heat transfer characteristics of nanofluids: A review, *Int. J. Therm. Sci.*, **2007**, 46, 1–19.
[4]. X. Q. Wang, A. S. Mujumdar, A review on nanofluids-part I: theoretical and numerical investigations, *Brazilian Journal of Chemical Engineering*, **2008**, 25(4), 613-630.
[5]. Y. Li, S. Tung, E. Schneider, S. Xi, A review on development of nanofluid preparation and characterization. *Powder technology*, **2009**, 196(2), 89-101.

[6]. S. Kakaç, A. Pramuanjaroenkij, Review of convective heat transfer enhancement with nanofluids. *International Journal of Heat and Mass Transfer*, **2009**, 52(13-14), 3187-3196.
[7]. S. P. Jang, S. U. Choi, Role of Brownian motion in the enhanced thermal conductivity of Nanofluids, *Applied physics letters*, **2004**, 84(21), 4316-4318.
[8]. R. Prasher, P. E. Phelan, P. Bhattacharya, Effect of aggregation kinetics on the thermal conductivity of nanoscale colloidal solutions (nanofluid), *Nano letters*, **2006**, 6(7), 1529-1534.
[9]. K. S. Gandhi, Thermal properties of nanofluids: controversy in the making? *Curr Sci*., **2007**, 92, 717–718
[10]. X. Li, D. Zhu, X. Wang, Evaluation on dispersion behavior of the aqueous copper nano-suspensions, *Journal of colloid and interface science*, **2007**, 310(2), 456-463.
[11]. A. Ravindran, A. Singh, A. M. Raichur, N. Chandrasekaran, A. Mukherjee, Studies on interaction of colloidal Ag nanoparticles with bovine serum albumin (BSA), *Colloids and Surfaces B: Biointerfaces*, **2010**, 76(1), 32-37.
[12]. N. Wangoo, K. K. Bhasin, S. K. Mehta, C. R. Suri, Synthesis and capping of water-dispersed gold nanoparticles by an amino acid: bioconjugation and binding studies, *Journal of colloid and interface science*, **2008**, 323(2), 247-254.
[13]. S. Liu, Y. Sui, K. Guo, Z. Yin, X. Gao, Spectroscopic study on the interaction of pristine C 60 and serum albumins in solution. *Nanoscale research letters*, **2012**, 7(1), 433.
[14]. Z. N. Gheshlaghi, G. H. Riazi, S. Ahmadian, M.Ghafari, R. Mahinpour, Toxicity and interaction of titanium dioxide nanoparticles with microtubule protein, *Actabiochimic aetbiophysicaSinica*, 2008, 40(9), 777-782.
[15]. T. Cedervall, I. Lynch, S. Lindman, T. Berggård, E. Thulin, H. Nilsson, S. Linse, Understanding the nanoparticle–protein corona using methods to quantify exchange rates and affinities of proteins for nanoparticles, *Proceedings of the National Academy of Sciences*, **2007**, 104(7), 2050-2055.
[16]. E. Fabian, R. Landsiedel, L. Ma-Hock, K. Wiench, W.Wohlleben, B.Van Ravenzwaay, Tissue distribution and toxicity of intravenously administered titanium dioxide nanoparticles in rats, *Archives of toxicology*, **2008**, 82(3), 151-157.
[17]. M. Lundqvist, I. Sethson, B. H. Jonsson, Protein adsorption onto silica nanoparticles: conformational changes depend on the particles' curvature and the protein stability. *Langmuir*, **2004**, 20(24), 10639-10647.
[18]. M. Lundqvist, I. Sethson, B. H. Jonsson, Transient interaction with nanoparticles “freezes” a protein in an ensemble of metastable near-native conformations, *Biochemistry*, **2005**, 44(30), 10093-10099.
[19]. E. Hellstrand, I. Lynch, A. Andersson, T. Drakenberg, B. Dahlbäck, K. A. Dawson, T. Cedervall, Complete high-density lipoproteins in nanoparticle corona, *The FEBS journal*, **2009**, 276(12), 3372-3381.
[20]. Z. Shervani, Y. Ikushima, M. Sato, H. Kawanami, Y. Hakuta, T. Yokoyama, K. Aramaki, Morphology and size-controlled synthesis of silver nanoparticles in aqueous surfactant polymer solutions. *Colloid and Polymer Science*, **2008**, 286(4), 403-410.
[21]. S. P. Boulos, T. A. Davis, J. A. Yang, S. E. Lohse, A. M. Alkilany, L. A. Holland, C. J. Murphy, Nanoparticle–protein interactions: a thermodynamic and kinetic study of the adsorption of bovine serum albumin to gold nanoparticle surfaces. *Langmuir*, **2013**, 29(48), 14984-14996.
[22]. W. H. Ho, C. F. Li, H. C. Liu, S. K. Yen, Electrochemical performance of In_2O_3 thin film electrode in lithium cell. *Journal of Power Sources*, **2008**, 175(2), 897-902.
[23]. S. K. Das, M. M. R. Khan, A. K. Guha, A. R. Das, A. B. Mandal, Silver-nanobiohybride material: synthesis, characterization and application in water purification. *Bioresource technology*, **2012**,124, 495-499.
[24]. R. Žūkienė, V. Snitka, (). Zinc oxide nanoparticle and bovine serum albumin interaction and nanoparticles influence on cytotoxicity in vitro. *Colloids and Surfaces B: Biointerfaces*, **2015**, 135, 316-323.